

## Experimental modal analysis of transverse-cracked rails- influence of the cracks on the real track behavior

Laura Montalbán Domingo<sup>\*1</sup>, Beatriz Baydal Giner<sup>1a</sup>, Clara Zamorano Martín<sup>2b</sup>  
and Julia I. Real Herráiz<sup>1c</sup>

<sup>1</sup>Department of Transportation Engineering and Infrastructures, School of Civil Engineering,  
Polytechnic University of Valencia, Camino de Vera 14, 46022 Valencia, Spain

<sup>2</sup>Foundation for the Research and Engineering in Railways, 160 Serrano, 28002 Madrid, Spain

(Received June 20, 2014, Revised August 2, 2014, Accepted August 20, 2014)

**Abstract.** Rails are key elements in railway superstructure since these elements receive directly the train load transmitted by the wheels. Simultaneously, rails must provide effective stress transference to the rest of the track elements. This track element often deteriorates as a consequence of the vehicle passing or manufacturing imperfections that cause in rail several defects. Among these rail defects, transverse cracks highlights and are considered a severe pathology because they can suddenly trigger the rail failure. This study is focused on UIC-60 rails with transverse cracks. A 3-D FEM model is developed in ANSYS for the flawless rail in which conditions simulating the crack presence are implemented. To account for the inertia loss of the rail as a consequence of the cracking, a reduction of the bending stiffness of the rail is considered. The numerical models have been calibrated using the first four bending vibration modes in terms of frequencies. These vibration frequencies have been obtained using the Experimental Modal Analysis technique, studying the changes in the modal parameters of the rails induced by the crack and comparing the results obtained by the model with experimental results. Finally, the calibrated and validated models for the single rail have been implemented in a complete railway ballasted track FEM model in order to study the static influence of the cracks on the rail deflection caused by a load passing.

**Keywords:** Experimental Modal Analysis (EMA); rail; transverse crack; finite element model (FEM)

### 1. Introduction

In the last decades, the study of the vibrations as Structural Health Monitoring (SHM) has been widely used to evaluate the actual state of the railway tracks. SHM often uses the Experimental Modal Analysis (EMA) as a fault detection procedure, as observed in the researches (Kaewunruen and Reminikov 2008, Reminikov and Kaewunruen 2008, Real *et al.* 2012) for the case of railway sleepers. The EMA method consists of the study of the variations in the dynamic properties of the structure as a consequence of the presence of structural damage. The dynamic properties of any

---

\*Corresponding author, Ph.D. Student, E-mail: [laumondo@cam.upv.es](mailto:laumondo@cam.upv.es)

<sup>a</sup>[beabaygi@cam.upv.es](mailto:beabaygi@cam.upv.es)

<sup>b</sup>[claraz@fundacioncdh.com](mailto:claraz@fundacioncdh.com)

<sup>c</sup>[jureaher@tra.upv.es](mailto:jureaher@tra.upv.es)

element are assessed according to the mass, stiffness and energy dissipation. Consequently, the presence of a crack will directly influence the natural frequencies, the damping parameters and the natural modes of vibration (i.e., modal parameters) (Acton A.C. 2008).

The experimental identification of the modal parameters is a research field with more than 6 decades of history. One of the most important milestones in this technique was achieved by Kennedy and Pancu (1947), who collected all the modal analysis information available back then. The fast development of the advances in electronic measurement and analysis procedures in the 1960s improved the accuracy of the measurements and thus, the scope of the method. Salter (1969) presented an interesting work in which a non-analytic approach was employed for the interpretation of the measured data. Nowadays, the Modal Analysis is a field widely studied by numerous researchers with a strong theoretical base documented in reference books (Ewins 2000, He and Fu 2001, Allemang and Brown 1987) and are applied as a procedure of structural evaluation (Salawu 1997).

Theoretically, Chalko *et al.* (1996) developed a new method of modal approximation (DSMA) able to calculate the modal parameters in data series with noise or when the modes are overlapped.

From the experimental approach, the Modal Analysis is extensively used in the detection, positioning and estimation of the severity of the crack in structural elements (Salawu 1997) thanks to the changes in the natural frequencies and vibration modes produced by the crack (Nahvi and Jabbari 2005). Yoo *et al.* (2006) used the Modal Analysis technique to determine the variation of the modal characteristics in a cantilever beam with a crack perpendicular to the neutral axis. To achieve that goal, the authors developed a procedure based on the Finite Element Method which allows estimating the variations in the modal properties in a precise manner. Wang *et al.* (2008) presented a new concept of EMA based on the study of the vibration responses of a structure. From the initial conditions, they created an algorithm to calculate the natural frequencies and the associated vibration modes from the displacements of the excited structure.

FEM models have been used to calculate the local flexibility in different studies in the last decade (Dirr and Schmalhorst 1988, Ostachowicz and Krawczuk 1990, Kaland and Rao 2012). The majority of the researches agree with the application of the analytic equations of the linear fracture mechanics in order to assess the local flexibility introduced by the crack, neglecting the effects that may affect the mass and the damping matrix (Nahvi and Jabbari 2005, Skrinar 2009).

The Modal Analysis applied to rails was initiated by Thompson (1993) who validated the EMA technique in this element, combining the results with basic FEM models of the rail. The same author studied a deeper analysis in three different tracks, exciting the vertical and transversal modes and achieving satisfactory results (Thompson 1997). In addition, Lanza di Scalea *et al.* (2004), Bartoli *et al.* (2005) used the EMA in rails to detect flaws and imperfections exciting the rails at high frequencies. Then, combining the EMA results with FEM models of the cracked rail, the transverse crack detection is justified by the results obtained.

As explained above, the EMA is a suitable methodology to the dynamic analysis of different structures. This paper presents the results of an Experimental Modal Analysis of a transversely cracked rail in lab conditions compared with an uncracked rail. Cracks are simulated by a cross-sectional incisions made with a radial cutting machine, simulating different fissure depths. The main purpose of the experiments is to assess the effects of the rail cracks on its dynamic behavior, depending on the different depths. To do so, the first four bending modes are analyzed and their variations, induced by the different cracks, studied. Experimental Modal Test results will be used to calibrate the 3D FEM models of the isolated flawed and undamaged rails. Subsequently, these models isolated rail models will be used to evaluate the structural influence of the rail cracks in a

FEM model of the whole track.

## 2. Modal analysis and structural cracking

### 2.1 Principles of experimental modal analysis

Experimental Modal Analysis is defined as the characterization process of the dynamic properties of a structural system. Within the dynamic properties, vibration modes, natural frequencies and damping factors are often considered.

EMA is based on the forced vibration test (FVT) that involves the measurement of dynamic excitations and their corresponding structural response. The relationship between the applied input and the observed output, which is known as Frequency Response Function (FRF), allows identifying the modal parameters.

$$H(\omega) = \frac{FFT(X(t))}{FFT(F(T))} = \frac{X(\omega)}{F(\omega)} \quad (1)$$

Where  $H(\omega)$  is the Frequency Response Function,  $X(\omega)$  and  $F(\omega)$  are the Fast Fourier Transform (FFT) of the vibration response  $X(t)$  of the system to the excitation force  $F(t)$ .

The values of response  $X(t)$  and excitation  $F(t)$  in the time domain, are extracted from Experimental Modal Test (EMT). The technique used in the rails EMT consists of an impact hammer excitation. This hammer induces a controlled excitation on the rail and the response is measured in terms of accelerations. The vibration time response of the structure is measured and then transformed to frequency domain using the Fast Fourier Transform algorithm. Since the magnitude of the force in frequency domain is controlled by the hammer, the Frequency Response Function (FRF) can be calculated. The quality of the results obtained from the EMA depends on the following technical aspects: the mechanical properties of the supports in the test and its position; the excitation method; the transducer elements and the signal processing techniques (Ewins 2000).

On the one hand, previous studies state that the transverse cracks tend to have a more significant influence on bending modes of vibrations than on twisting modes (Thompson 1993). On the other hand, bending is the most important effect in rail (Thompson 2009). Consequently, the present work focuses on the unbounded bending behavior of the rails.

### 2.2 Implications of cracking

The use of mechanical vibrations in modal analysis is a very useful technique for structural diagnosis. This assertion implies that the presence of cracks has strong influence on the stiffness. However, the mass loss as a consequence of the cracking is negligible. This stiffness variation in the crack surroundings will alter the modal parameters, specially the natural frequencies (Kaland and Rao 2012).

The variations in the Frequency Response Function (FRF) measured in terms of displacement, velocity or acceleration reflect the alteration of the rail natural frequencies as a consequence of the cracks.

The present research analyzes the crack influence on the dynamic parameters in terms of the natural frequencies of the first four bending modes of isolated rail. As explained before, these



Fig. 1 Experimental modal test setup

natural frequencies variation depend only on the stiffness decrease caused by the crack, which affects both the static and dynamic behavior of rails.

### 3. Experimental tests

#### 3.1 Experiment scope

Experimental Modal Test is performed on four 1.5 m long UIC-60 specimens to obtain the required data for the calibration of the finite element models. One of the rails tested is undamaged and the other three have been cracked with a radial saw at a distance of 0.7 m from one of the tops. Cracks are 5 mm thick and each one of the cracked rails has a different fissure depth. In this manner, the influence of the crack depth on the eigenmodes' frequencies can be studied. The depths of the fissures in the cracked rails studied are 0.022, 0.043 and 0.098 m.

#### 3.2 Experimental modal test: data collection

Impact hammer excitation technique was used to evaluate the natural frequencies. The instruments used in this study, which are shown in Fig. 1, were the impact hammer to excite the rails, four triaxial accelerometers to register vibration data and the software required to register the results in a laptop. Results obtained from the test are in the time domain. Therefore, Matlab algorithms were designed for the post-processing of the measured data in order to obtain the Frequency Response Functions (FRFs).

Test design was previously studied in a FEM model of the rail in order to know the distribution of the vibrations modes of the first four bending modes of vibration. The nodes, where the amplitude of the different vibration modes is zero (Wolf 1991a, b, 1994), were calculated with this previous FEM model. For simulating the free boundary conditions, two rubber supports were used. The location of this support matches the position of the nodes obtained from the previous analysis. In this manner, the rubber supports do not alter the stiffness of the rail and the response obtained corresponds to the real response of the isolated rail (Carne *et al.* 2007). In previous researches, the suitability of recycled rubber supports for modal testing was evidenced (Real *et al.* 2012,

Table 1 Experimental frequencies of vibration (Hz)

|                            | F <sub>1</sub> 1 <sup>st</sup> bending mode (Hz) | F <sub>2</sub> 2 <sup>nd</sup> bending mode (Hz) | F <sub>3</sub> 3 <sup>rd</sup> bending mode (Hz) | F <sub>4</sub> 4 <sup>th</sup> bending mode (Hz) |
|----------------------------|--|--|--|--|
| Undamaged rail             | 466.009  | 1090.400   | 1797.780   | 2497.070   |
| 0.022 m depth cracked rail | 462.968  | 1087.040   | 1792.470   | 2488.020   |
| 0.043 m depth cracked rail | 460.360  | 1083.374   | 1786.100   | 2478.899   |
| 0.098 m depth cracked rail | 408.450  | 1032.409   | 1718.820   | 2334.250   |

Montalbán *et al.* 2014).

From the previous FEM model, the optimal excitation and measurement points can be placed in the position where the first four bending modes were developed. Since the vertical bending is studied, both accelerometers and impact points are located on the rail surface. In the essay, two different points were excited to confirm the Maxwell Reciprocity hypothesis which asserts that the response in the Experimental Modal Test does not depend on the impact point.

### 3.3 Results

The frequencies obtained from the Experimental Modal Analysis are shown in Table 1. This table collects the first four bending modes of vibration of the rails in terms of frequency. The Frequency Response Function has been obtained from the signal processing using the FFT in Matlab to convert the measured results in time domain to frequency domain. Once FRFs are obtained and using the Peak-Picking Method for modal parameters identification, the peaks of FRF which determine each modal frequency can be calculated (Ren and Zong 2003).

From the results obtained in the previous table, it can be seen how the presence of cracks decreases the frequency of the natural modes, as expected in damaged structures.

## 4. Finite element modelling of the rail

### 4.1 FEM of the undamaged rail

The rail is an element whose behavior can be assimilated to a bending beam. Considering the Timoshenko beam theory (Félix *et al.* 2009), it is possible to analyze the influence of the parameters governing the characteristics of the bending modes according to the following equation

$$\omega_n = n^2 \pi^2 \sqrt{\frac{EI}{\rho AL^4}} \quad (2)$$

Where  $\omega_n$  is the natural frequency of the n-mode,  $n$  is the order of the bending mode,  $E$  is the Young's modulus,  $I$  is the inertia of the rail section,  $\rho$  is the density of the steel,  $A$  is the cross section area and  $L$  is the length of rail.

The FEM model developed must represent the natural frequencies of vibration obtained in the experimental test conditions and also simulate the rail real behavior under static loading in order to

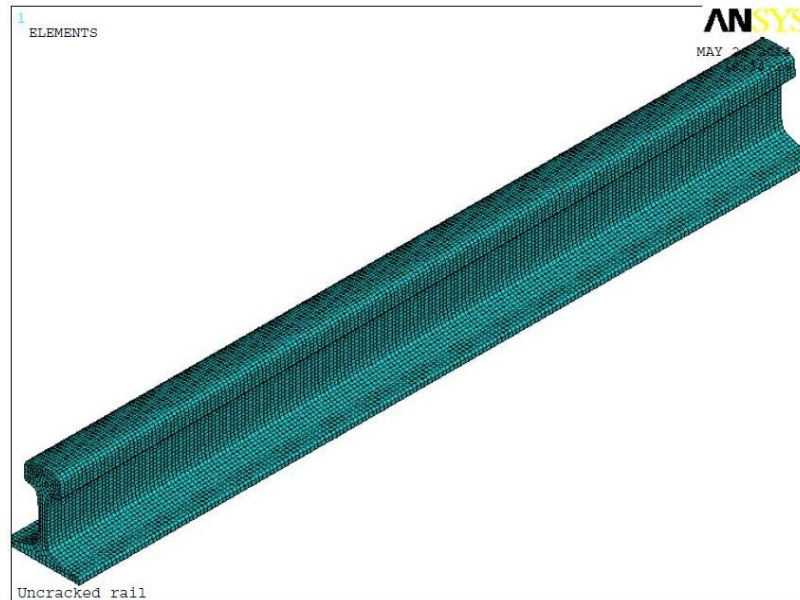


Fig. 2 FEM model of the undamaged rail

study the complete railway track model.

Rail geometry depicted in Fig. 2 corresponds to 1.5 m long UIC-60 normalized profile rails. The mechanical properties required for a modal analysis using finite element method are the elastic modulus, Poisson's ratio and the density of the rail. The rail is divided into brick elements SOLID95 and the edge of the elements is 5 mm.

#### 4.2 FEM of the cracked rail

Once the model of the undamaged rail has been correctly developed, it is necessary to introduce some modifications that simulate the effect of the crack in the model. In order to introduce these modifications, it is necessary to understand which consequences the presence of a crack has on the structure behavior: a crack is a discontinuity in the material that introduces a decrease in the cross section inertia.

The modeling assumes that the presence of a crack only affects to the moment of inertia of the cracked rail section (Nahvi and Jabbari 2005, Skrinar 2009). This decrease in inertia also decreases the flexural rigidity, which is defined as the product between the inertia and the elasticity modulus.

$$\text{FlexuralRigidity} = EI \quad (3)$$

In finite elements, the modeling of crack as a gap is not feasible because this gap induces calculation errors as a consequence of its small dimensions. A continuous rail section with larger dimensions than the actual gap is modeled instead. Since the inertia cannot be modified because the geometry of the model is maintained, the loss of flexural stiffness effect can be achieved by introducing a reduction of the Young's modulus in the area where the fissure appears (Bovsunivsky and Matveev 2000). In conclusion, the crack is simulated as a volume of flexible material embedded in a rail cross section as shown in Fig. 3.

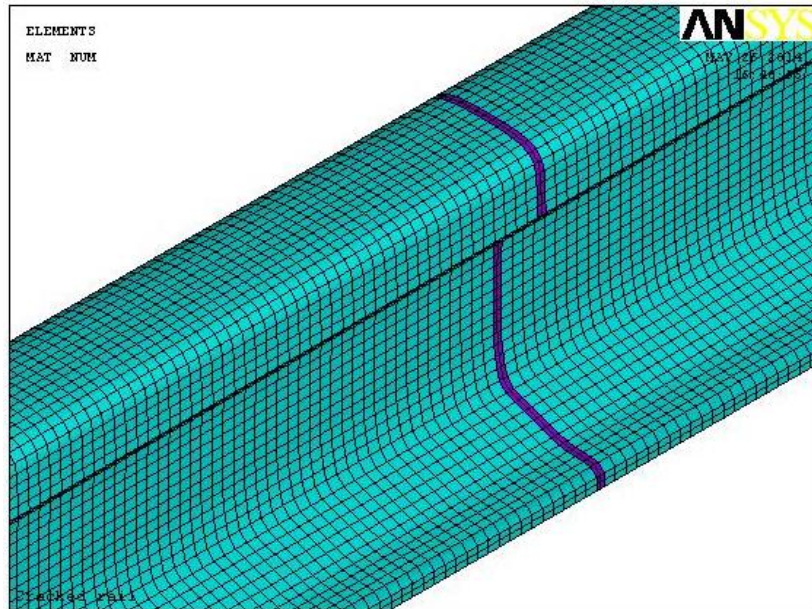


Fig. 3 FE model of the cracked rail. Crack is represented by the purple section

The parameters of the new material accounting for the effect of the crack must be calibrated. The calibration ensures that the behavior of the rail with the flexible material inserted is the same as the real cracked rail; the comparison between experimental and FEM model results is done on the basis of the natural frequencies in Table 1. The unknown values which must be calibrated are the Young's modulus of the filling material and the crack thickness (Isernia and Rodríguez 2011). The rest of the mechanical properties of the crack material (i.e., density and Poisson's ratio) are assumed equal to those of the rail steel. Assaying different combinations of these two parameters, different natural frequencies are obtained and comparing these frequencies with the results obtained in the real tests, the optimal combination of the values of thickness and Young's modulus is obtained for each cracked rail.

#### 4.3 Results- model calibration

All the calculations have been performed using the Modal Analysis tool provided by ANSYS v11.0, which solves the free undamped vibration equation

$$\text{Dynamics equation (undamped)} \\ M\ddot{u} + Ku = 0 \quad (4)$$

Where  $M$  is the mass matrix,  $K$  is the stiffness matrix,  $u$  is the displacement vector, and  $\ddot{u}$  the acceleration vector. This analysis neglects the damping, which is suitable for this study since it only affects to the energy dissipation but not to the value of the frequencies (Nahvi and Jabbari 2005, Skrinar 2009). Consequently, the natural frequencies of the undamped structure can be calculated according to the undamped dynamics equation in Eq. (4).

As explained in section 4.2, the calibration is done by changing the crack thickness and the

Table 2 Mechanical properties of modeled rails

|                               | Young's modulus<br>undamaged rail (N/m <sup>2</sup> ) | Young's modulus<br>cracked section (N/m <sup>2</sup> ) | Density<br>(kg/m <sup>3</sup> ) | Crack<br>thickness (m) | Poisson's<br>ratio |
|-------------------------------|---|--|---------------------------------|------------------------|--------------------|
| Undamaged rail                | 2.1E11  | ---  | 7850                            | ---                    | 0.3                |
| 0.022 m depth<br>cracked rail | 2.1E11  | 1.4645E11  | 7850                            | 0.015                  | 0.3                |
| 0.043 m depth<br>cracked rail | 2.1E11  | 1.06E11  | 7850                            | 0.018                  | 0.3                |
| 0.098 m depth<br>cracked rail | 2.1E11  | 0.45E11  | 7850                            | 0.057                  | 0.3                |

Table 3 Experimental and model results for the undamaged rail-errors

|                                | F <sub>1</sub> 1 <sup>st</sup> bending<br>mode (Hz) | F <sub>2</sub> 2 <sup>nd</sup> bending<br>mode (Hz) | F <sub>3</sub> 3 <sup>rd</sup> bending<br>mode (Hz) | F <sub>4</sub> 4 <sup>th</sup> bending<br>mode (Hz) |
|--------------------------------|---|---|---|---|
| Experimental                   | 466.009   | 1090.400  | 1797.780  | 2497.070  |
| Model                          | 466.010   | 1090.490  | 1796.960  | 2497.210  |
| % Error                        | -0.0013%  | -0.0082%  | 0.046%  | -0.0056%  |
| $\sqrt{\Sigma \text{Error}^2}$ | 0.0047 %  |   |   |   |

Table 4 Experimental and model frequencies of the cracked rail at 0.022 m-errors

| 0.022 m depth<br>cracked rail  | F <sub>1</sub> 1 <sup>st</sup> bending<br>mode (Hz) | F <sub>2</sub> 2 <sup>nd</sup> bending<br>mode (Hz) | F <sub>3</sub> 3 <sup>rd</sup> bending<br>mode (Hz) | F <sub>4</sub> 4 <sup>th</sup> bending<br>mode (Hz) |
|--------------------------------|---|---|---|---|
| Experimental                   | 462.968   | 1087.040  | 1792.470  | 2488.020  |
| Model                          | 463.338   | 1087.065  | 1791.567  | 2488.841  |
| Error                          | - 0.0799%   | - 0.0023%   | 0.0504%   | - 0.033%  |
| $\sqrt{\Sigma \text{Error}^2}$ | 0.1 %   |   |   |   |

Table 5 Experimental and model frequencies of the cracked rail at 0.043 m-errors

| 0.043 m depth<br>cracked rail  | F <sub>1</sub> 1 <sup>st</sup> bending<br>mode (Hz) | F <sub>2</sub> 2 <sup>nd</sup> bending<br>mode (Hz) | F <sub>3</sub> 3 <sup>rd</sup> bending<br>mode (Hz) | F <sub>4</sub> 4 <sup>th</sup> bending<br>mode (Hz) |
|--------------------------------|---|---|---|---|
| Experimental                   | 460.360   | 1083.374  | 1786.100  | 2478.899  |
| Model                          | 459.707   | 1083.351  | 1786.082  | 2479.926  |
| Error                          | -0.1418%  | 0.0022%   | 0.001 %   | - 0.0414 %  |
| $\sqrt{\Sigma \text{Error}^2}$ | 0.14 %  |   |   |   |

Young's modulus of the crack material and then comparing the results obtained with those coming from the experimental tests. In Table 2, results of the calibration process are shown for the three cracked rails.

Results of the modal analysis processed by ANSYS for the undamaged rail are shown in Table 3. As can be observed, the difference between results of the finite element models and the experimental measurements are minimal. Errors are very small so that the correlation between experimental and modeled data is ensured.

Differences between the experimental and the model results after calibration are also minimal. In the Tables 4-6, results corresponding to different crack depths are displayed.

Table 6 Experimental and model frequencies of the cracked rail at 0.098 m-errors

| 0.098 m depth cracked rail     | F <sub>1</sub> 1 <sup>st</sup> bending mode (Hz) | F <sub>2</sub> 2 <sup>nd</sup> bending mode (Hz) | F <sub>3</sub> 3 <sup>rd</sup> bending mode (Hz) | F <sub>4</sub> 4 <sup>th</sup> bending mode (Hz) |
|--------------------------------|--|--|--|--|
| Experimental                   | 408.450  | 1032.409   | 1718.820   | 2334.250   |
| Model                          | 408.327  | 1032.481   | 1717.296   | 2334.828   |
| Error                          | 0.0301%  | 0.005%   | 0.0887 %   | -0.0234 %  |
| $\sqrt{\Sigma \text{Error}^2}$ | 0.3 %  |  |  |  |

#### 4.4 Discussion of results

Finite element models of the cracked rails accurately represent the variations in the natural frequencies of the bending modes observed in the real tests. The cracked rail values result perfectly defined by changing the Young modulus and the thickness of the cracked section. When the crack is deeper, the flexural rigidity of that section is reduced and therefore the resulting calibrated values of Young's modulus decrease and crack thickness increase to compensate the bending stiffness loss.

It can be stated that the approach presented to account for cracked and undamaged rails in finite elements model is suitable. The bending behavior of the rails is perfectly simulated and therefore the rails can be implemented in a complete track FEM model.

### 5. Application to ballasted track

#### 5.1 FE track model

In order to reproduce the real behavior of a track against vertical stresses, a 3D finite elements model of a ballasted track is created. In this model, the track response when using both cracked and undamaged rails will be studied. The railway FE modeling has been performed according to the work collected by the D-117 ORE technical committee (Profillidis 1986, Shanin 2008) and the recommendations for the project to rail infrastructure developed by Spanish Ministry of Public Works (Recomendaciones para el proyecto de plataformas ferroviarias 1999)

The domain of track cross section is the suitable for a high speed track according to IGP-2008 (Instrucciones Generales para los Proyectos de la Plataforma 2008). The longitudinal extension of the model is calculated on the basis of Pandolfo theory. This theory asserts that a load on the rail affects up to 4 adjacent sleepers in each direction. Symmetry of the cross section, as depicted in Fig. 4, has been considered to simplify the calculations thus reducing the computing time.

The geometry of the rail has been previously developed in the isolated rail models. The rail pad and the sleeper AI-04-EA were modeled with an equivalent geometry, maintaining the bending stiffness of each element (Gallego 2006, Gallego *et al.* 2009, Gallego *et al.* 2011, Isernia and Rodríguez 2011). For these three components, linear-elastic constitutive model of the materials is assumed. On the other hand, for ballast layer, subgrade, embankment and track foundation an elastoplastic behavior based on the Drucker Prager model is assumed (Drucker and Prager 1952, Profillidis 1986). The mechanical properties of the rail pad, ballast, subgrade and underlying layers were known for the modeled high speed track. The element used for the representation of the modeled volume is, as in the case of isolated rail, the SOLID 95 brick element with 20-nodes. This

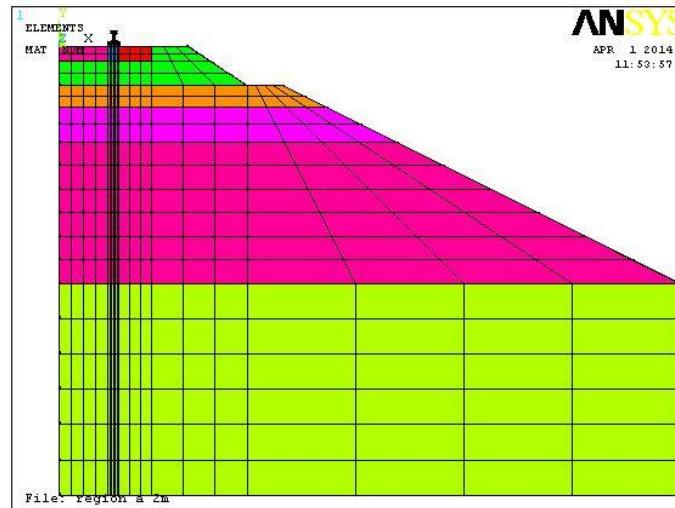


Fig. 4 Half cross-section track model

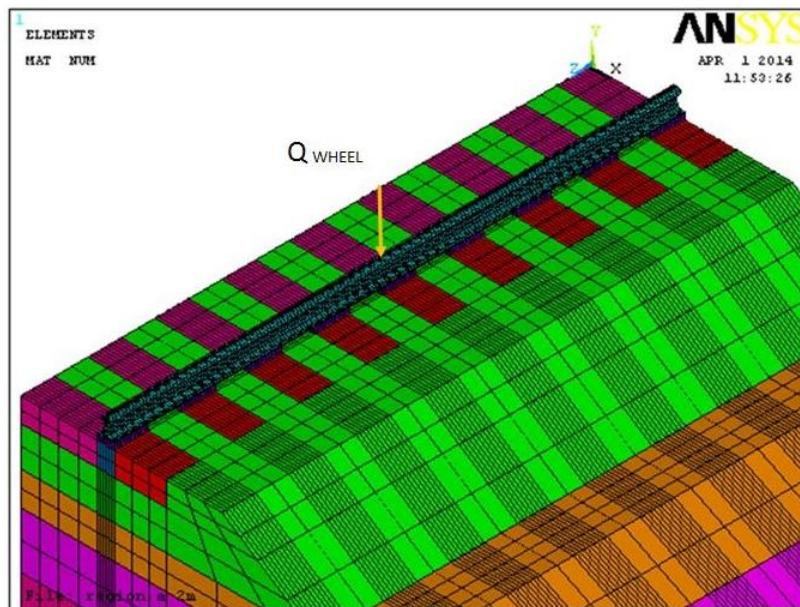


Fig. 5 FEM track model

element is recommended to model sections under bending stresses (Isernia and Rodríguez 2011). The longitudinal mesh size is 0.03 m on sleepers and 0.3 m between them.

To calibrate and validate the whole high speed track model with undamaged rails, real measurements of vertical deflections from a ballasted track in Spain have been used. The vertical load transmitted by the wheels and represented in Fig. 5 by a yellow arrow, has been calculated according to Eisenmann (Giannakos 2010, Montalbán *et al.* 2012, Teixeira 2003) to include the dynamic overloads.

Table 7 Head rail deflections in the track model

|                            | Loading and crack<br>on rail support (m) | % $\Delta$ | Loading and crack<br>between rail support (m) | % $\Delta$ |
|----------------------------|--|------------|---|------------|
| Undamaged rail             | -0,00123547                              | 100        | -0,00127023                                   | 100        |
| 0.022 m depth cracked rail | -0.00125335                              | 101.45     | -0,00130192                                   | 102.5      |
| 0.043 m depth cracked rail | -0.0012705                               | 102.83     | -0,00131953                                   | 103.98     |
| 0.098 m depth cracked rail | -0,00138075                              | 111.76     | -0,00148995                                   | 117.3      |

## 5.2 FEM track model results

In order to calculate the response of the track with damaged rails, two different positions of the cracks are studied: over the support and in the middle point between supports. The load is applied in every case on the cracked section and the corresponding results of the deflections measured at the rail head are shown in Table 7. A comparison is established between the undamaged rail and the different cracked rails.

## 5.3 Discussion of results

As seen in the single rail model, cracking creates a stiffness reduction in the cracked area. Consequently, this section is more flexible and the loads cause higher strains and as shown in Table 7, the deflections grow with the crack depth.

According to Table 7, differences between deflections corresponding to 2.2 and 4.3 cm of crack depth are not significant. However, when the crack reaches the rail web with a depth of 9.8 cm, deflections increase by 12% when the crack is located above the rail support and by 17% if the crack is in the middle span compared to the non-cracked situation. Thus, the more adverse situation is when the crack is located between two supports and may lead to the sudden failure of the structure.

Apart from the sudden breakage of the rail, when the deflections of the rail head increase, so do the deflections in other elements beneath the rail. This fact means increased stresses which may compromise the stability of the track. The presence of a gap in the rail as a consequence of a crack also produces higher dynamic overloads, not only in the rail but also in the vehicle.

Finally, the modification of the modal parameters of the track must be considered. The damping track is increased by the crack and therefore resonance phenomena may appear in the vehicle. Resonance brings with a decrease in the passenger comfort and a high deterioration of the track and the vehicles as well.

## 6. Conclusions

Three dimensional Finite Element models for the undamaged and cracked rails have been successfully developed. Models are able to faithfully predict the modal response against a controlled excitation.

The correct simulation of the free-vibration condition with the elastomeric bases in the nodes of the natural modes is suitable since it does not alter the results of the experimental campaign.

The minimum errors obtained after the calibration process reveal that the combined

methodology consisting of EMA (where damping is neglected) and FEM model yields accurate results. Thus, cracks can be represented in terms of elasticity modulus and crack thickness in the FEM model reproducing the real conditions.

Three dimensional models of railway tracks containing cracked rails have revealed that the location of the rail crack between supports produces higher deflections at the rail head than a crack located over the supports. The first situation is thus more unfavorable than the second because the durability of the infrastructure may be compromised. In addition, excessive deflections of the rail head may affect the travelers comfort and induce noise and vibration.

The conclusions stated above have been obtained from theoretical cracks which do not appear in real rails. However, results obtained constitute a first approach of the behavior of the rails with real cracks.

## References

- Acton, A.C. (2008), "Clustering results around peaks for full-harmonic analyses in ANSYS", ANSYS Incorporation.
- Allemang, R.J. and Brown, D.L. (1987), *Experimental modal analysis and dynamic component synthesis*, Air force wright aeronautical laboratories, EE. UU.
- Bartoli, I., Lanza di Scalea, F., Fateh, M. and Viola, E. (2005), "Modeling guided wave propagation with application to the long-range defect detection in railroad tracks", *NDT Int.*, **38**, 325-334.
- Bovsunovsky, P. and Matveev, V.V. (2000), "Analytical approach to the determination of dynamic characteristics of beam with a closing crack", *J. Sound Vib.*, **235**, 415-434.
- Carne, T., Todd, D. and Casias, M. (2007), "Support conditions for free boundary-condition modal testing", *IMAC XXV, the 25th International Modal Analysis Conference*, Orlando, FL, February.
- Chalko, T.J., Haritos, N. and Gershkovich, V. (1996), "Non-linear curve fitting for modal analysis", *Environ. Softw.*, **11**(1-3), 9-18.
- Dirr, B.O. and Schmalhorst, B.K. (1988), "Crack depth analysis of a rotating shaft by vibration measurements", *ASME J. Vib. Acoust.*, **110**, 158-164.
- Drucker, D.C. and Prager, W. (1952), "Soil mechanics and plastic analysis or limit design", *Quart. Appl. Math.*, **10**, 157-65.
- Ewins, D.J. (2000), *Modal testing: Theory and Practice*, Research Studies Press, London, UK.
- Félix, D., Rossi, R. and Bambill, D. (2009), "Análisis de vibración libre de una viga Timoshenko escalonada, centrifugamente rigidizada, mediante el método de la cuadratura diferencial", *Revista Internacional de Métodos Numéricos para Cálculo y diseño en Ingeniería*, **25**, 111-132. (in Spanish)
- Gallego, I. (2006), "Heterogenidad resistente de las vías de alta velocidad: transición terraplén-estructura", PhD Thesis, Universidad de Castilla-La Mancha, Ciudad Real. (in Spanish)
- Gallego, I. and López, A. (2009) "Numerical simulation of embankment-structure transition design", *J. Rail Rapid Tran.*, **223**(4), 331-343.
- Gallego, I., Muñoz, J., Rivas, A. and Sanchez-Cambronero, S. (2011) "Vertical track stiffness as a new parameter involved in designing high-speed railway infrastructure", *J. Tran. Eng.*, **137**, 971-979.
- Giannakos, K. (2010), "Influence of rail pad stiffness on track stressing, life-cycle and noise emission. second international conference on sustainable construction materials and technologies", *Special Technical Proceedings*, Università Politecnica delle Marche, Ancona, Italy, June.
- He, H. and Fu, Z. (2001), *Modal Analysis*, Great Britain Butterworth - Heinemann Publishers, Oxford, UK.
- IGP (2008), *Instrucciones Generales para los Proyectos de la Plataforma*, Spain. (in Spanish)
- Isernia-Trebols, D.J. and Rodríguez-Matienzo, J. (2011), "El modelado de una grieta de fatiga en una estructura plana y su detección mediante la transformada wavelet", *Revista Ingeniería Mecánica*, **14**, 74-86. (in Spanish)

- Kaewunruen, S. and Reminnikov, A.M. (2008), "Dynamic effect on vibrations signatures of cracks in railway prestressed concrete sleepers", *Adv. Mater. Res.*, **41-42**, 233-239.
- Kaland, A. and Rao, B.N. (2012), "Two-dimensional elastic-plastic cracked finite element for fracture applications", *Indian J. Eng. Mater.*, **19**, 95-106.
- Kennedy, C. and Pancu, C. (1947), "Use of vectors in vibration measurement and analysis", *J. Aeronaut. Sci.*, **14**(11), 603-625.
- Lanza di Scalea, F. and McNamara, J. (2004), "Measuring high-frequency wave propagation in railroad tracks by joint time-frequency analysis", *J. Sound Vib.*, **273**, 637-651.
- Ministerio de fomento/Secretaria de estado de Infraestructuras y transportes (1999), *Recomendaciones para el proyecto de plataformas ferroviarias*, Centro de publicaciones, Spain. (in Spanish)
- Montalbán, L., Real, J. and Real, T. (2012), "Mechanical characterization of railway structures based on vertical stiffness analysis and railway structures stress state", *J. Rail Rapid Tran.*, **227**(1), 74-85.
- Montalbán, L., Zamorano, C., Palenzuela, C. and Real, J.I. (2014), "Finite element modelling of cracked railway pre-stressed concrete sleepers", *Eur. J. Environ. Civil Eng.*, DOI 10.1080/19648189.2014.935486.
- Nahvi, H. and Jabbari, M. (2005), "Crack detection in beams using experimental modal data and finite element model", *Int. J. Mech. Sci.*, **47**, 1477-1497.
- Ostachowicz, W.M. and Krawczuk, M. (1990), "Vibration analysis of a cracked beam", *Comput. Struct.*, **36**(2), 245-50
- Profillidis, V. (1986), "Applications of finite element analysis in the rational design of track bed structures", *Comput. Struct.*, **22**(3), 439-443.
- Real, J.I., Sánchez, M.E., Real, T., Sánchez, F.J. and Zamorano, C. (2012), "Experimental modal analysis of railway concrete sleepers with cracks", *Struct. Eng. Mech.*, **44**(1), 51-60.
- Real, J.I., Gómez, L., Montalbán, L. and Real, T. (2012), "Study of the influence of geometrical and mechanical parameters on ballasted railway tracks design", *J. Mech. Sci. Techn.*, **26**(9), 2837-2844.
- Remennikov, A.M. and Kaewunruen, S (2008), "A review on loading condition of railway track structures due to wheel and rail vertical interactions", *Struct. Control Hlth. Monit.*, **15**, 207-234.
- Ren, W.X. and Zong, Z.H. (2003), "Output-only modal parameter identification of civil engineering structures", *Struct. Eng. Mech.*, **17**(3-4), 429-444.
- Salawu, O.S. (1997), "Detection of structural damage through changes in frequency: a review", *Eng. Struct.*, **19**(9), 718-723.
- Salter, J.P. (1969), *Steady State Vibration*, Kenneth Mason Press.
- Shanin, M. (2008), "Investigation into some design aspects of ballasted railway track substructure. Conference on railway engineering", *Earthworks and track bed construction for railway lines, UIC 719, International Union of Railways*, Perth, September.
- Skrinar, M. (2009), "Elastic beam finite element with an arbitrary number of transverse cracks", *Finit. Elem. Anal. Des.*, **45**(3), 181-189.
- Texeira, P.F. (2003), "Contribución a la reducción de los costes de mantenimiento de vías de alta velocidad mediante la optimización de la rigidez vertical", PhD Thesis, Universitat Politècnica de Catalunya, Barcelona. (in Spanish)
- Thompson, D. (1993), "Wheel-rail noise generation, Part III: rail vibration", *J. Sound Vib.*, **161**(3), 421-446
- Thompson, D. (1997), "Experimental analysis of wave propagation in railway tracks", *J. Sound Vib.*, **203**(5), 867-888.
- Thompson, D. (2009), *Railway Noise and Vibration: Mechanisms, Modelling and Means of Control*, Elsevier, Oxford, UK.
- Wang, B.T. and Cheng, D.K. (2008), "Modal analysis of mdof system by using free vibration response data only", *J. Sound Vib.*, **311**(3-5), 737-55
- Wolf, J.P. (1991a), "Consistent lumped-parameter models for unbounded soil: physical presentation", *Earthq. Eng. Struct. Dyn.*, **20**, 11-32.
- Wolf, J.P. (1991b), "Consistent lumped-parameter models for unbounded soil: frequency-independent stiffness, damping and mass matrices", *Earthq. Eng. Struct. Dyn.*, **20**, 33-41.
- Wolf, J.P. (1994), *Foundation Vibration Using Simple Physical Models*, PTR Prentice-Hall, Inc., New

Jersey, U.S.A.

Yoo, H.H., Cho, J.E. and Ching, J.T. (2006), "Modal analysis and shape optimization of rotating cantilever beams", *J. Sound Vib.*, **290**(1-2), 223-41.

CC